A peer-reviewed version of this preprint was published in PeerJ on 4 September 2018.

View the peer-reviewed version (peerj.com/articles/5524), which is the preferred citable publication unless you specifically need to cite this preprint.

Wang Z, Dou M, Liu F, Jiang P, Ye S, Ma L, Cao H, Du X, Sun P, Su N, Lin F, Zhang R, Li C. 2018. GDF11 induces differentiation and apoptosis and inhibits migration of C17.2 neural stem cells via modulating MAPK signaling pathway. PeerJ 6:e5524 https://doi.org/10.7717/peerj.5524

GDF11 induces differentiation and apoptosis and inhibits migration of C17.2 neural stem cells via modulating MAPK signaling pathway

Zongkui Wang [1], **Miaomiao Dou** [1], **Fengjuan Liu** [1], **Peng Jiang** [1], **Shengliang Ye** [1], **Li Ma** [1], **Haijun Cao** [1], **Xi Du** [1], **Pan Sun** [1], **Na Su** [1], **Fangzhao Lin** [1], **Rong Zhang** [Corresp., 1], **Changqing Li** [Corresp. 1]

[1] Institute of Blood Transfusion, Chinese Academy of Medical Sciences&Peking Union Medical College, Chengdu, Sichuan, China

Corresponding Authors: Rong Zhang, Changqing Li
Email address: kylie2009@foxmail.com, lichangqing268@163.com

GDF11, a member of TGF-β superfamily, has recently received widespread attention as a novel anti-ageing/rejuvenation factor to reverse age-related dysfunctions in heart and skeletal muscle, and to induce angiogenesis and neurogenesis. However, these positive effects of GDF11 were challenged by several other studies. Furthermore, the mechanism is still not well understood. In the present study, we evaluated the effects and underlying mechanisms of GDF11 on C17.2 neural stem cells. GDF11 induced differentiation and apoptosis, and suppressed migration of C17.2 neural stem cells. Besides, GDF11 slightly increased cell viability after 24h treatment, showed no effects on proliferation for about 10 days of cultivation, and slightly decreased cumulative population doubling for long-term treatment ($p<0.05$). Phospho-proteome profiling array displayed that GDF11 significantly increased the phosphorylation level of 13 serine/threonine kinases ($p<0.01$), including p-p38, p-ERK and p-Akt, in C17.2 cells, which implied the activation of MAPK pathway. Western blot validated that the results of phospho-proteome profiling array were reliable. Based on functional analysis, we demonstrated that the differentially expressed proteins were mainly involved in signal transduction which was implicated in cellular behavior. Collectively, our findings suggest that, for neurogenesis, GDF11 might not be the desired rejuvenation factor, but a potential target for pharmacologic blockade.

GDF11 induces differentiation and apoptosis and inhibits migration of C17.2 neural stem cells via modulating MAPK signaling pathway

Zongkui Wang[1], Miaomiao Dou[1], Fengjuan Liu[1], Peng Jiang[1], Shengliang Ye[1], Li Ma[1], Haijun Cao[1], Xi Du[1], Pan Sun[1], Na Su[1], Fangzhao Lin[1], Rong Zhang[1*], Changqing Li [1*]

[1]Institute of Blood Transfusion, Chinese Academy of Medical Sciences & Peking Union Medical College, Chengdu, China, 610052

*** Corresponding authors**:

Rong Zhang, e-mail: kylie2009@foxmail.com;
Changqing Li, e-mail: lichangqing268@163.com.

Abstract

GDF11, a member of TGF-β superfamily, has recently received widespread attention as a novel anti-ageing/rejuvenation factor to reverse age-related dysfunctions in heart and skeletal muscle, and to induce angiogenesis and neurogenesis. However, these positive effects of GDF11 were challenged by several other studies. Furthermore, the mechanism is still not well understood. In the present study, we evaluated the effects and underlying mechanisms of GDF11 on C17.2 neural stem cells. GDF11 induced differentiation and apoptosis, and suppressed migration of C17.2 neural stem cells. Besides, GDF11 slightly increased cell viability after 24h treatment, showed no effects on proliferation for about 10 days of cultivation, and slightly decreased cumulative population doubling for long-term treatment ($p<0.05$). Phospho-proteome profiling array displayed that GDF11 significantly increased the phosphorylation level of 13 serine/threonine kinases ($p<0.01$), including p-p38, p-ERK and p-Akt, in C17.2 cells, which implied the activation of MAPK pathway. Western blot validated that the results of phospho-proteome profiling array were reliable. Based on functional analysis, we demonstrated that the differentially expressed proteins were mainly involved in signal transduction which was implicated in cellular behavior. Collectively, our findings suggest that, for neurogenesis, GDF11 might not be the desired rejuvenation factor, but a potential target for pharmacologic blockade.

Keywords

Growth differentiation factor 11; C17.2 neural stem cells; differentiation; apoptosis; migration; MAPK signaling pathway

1. Introduction

Growth differentiation factor 11 (GDF11), also known as bone morphogenetic protein 11 (BMP11), is a secreted glycoprotein belonging to the transforming growth factor β (TGF-β) superfamily(Pepinsky et al. 2017; Walker et al. 2016). GDF11 plays an important role in anterior/posterior axial patterning during embryonic development(Oh et al. 2002). Similar to the negative effect of myostatin (also known as GDF8, which is 90% homology with GDF11(Walker et al. 2017)) in skeletal muscle, GDF11 acts as a negative regulator of neurogenesis in the olfactory epithelium(Wu et al. 2003) and the developing spinal cord(Santos et al. 2012).

Recently, Loffredo et al. suggested that GDF11 was the rejuvenation factor to reverse age-related dysfunction in heart(Loffredo et al. 2013). Subsequently, it was confirmed that GDF11 induced repairment of skeletal muscle and improvement of cognitive function(Katsimpardi et al. 2014; Sinha et al. 2014). However, the positive effects of GDF11 on heart, skeletal muscle and brain were questioned by a couple of independent studies. Egerman and colleagues(Egerman et al. 2015) discovered GDF11 supplementation inhibited muscle regeneration and decreased satellite cell expansion in mice, and implied that GDF11was not a rejuvenation factor but a potential target for pharmacologic blockade to treat age-related sarcopenia. Hinken et al.(Hinken et al. 2016) also suggested GDF11 wasn't a rejuvenator of aged murine skeletal muscle satellite cells. In addition, others reported restoring GDF11 in old mice had no effect on cardiac structure or function(Smith et al. 2015). These conflicting studies offer compelling evidence that the effects of GDF11 are contradictory and demonstrate that the effects of GDF11 on neurogenesis are still not completely understood. Therefore, we require an in-depth knowledge of the effects and potential mechanism of action of GDF11 on regulating neural stem cells.

In the present study, we focused on the effects of GDF11 on the cellular behavior of C17.2 neural stem cells (including viability, proliferation, differentiation, apoptosis and migration), the changes in the phospho-proteome and the corresponding signaling pathways. We herein showed that GDF11 promoted differentiation and apoptosis, and suppressed migration of C17.2 cells. Besides, GDF11 induced cellular proliferation in a short time, however it inhibited proliferation in a long-term cultivation. Pathway-oriented proteome profiling revealed that GDF11 stimulation significantly activated phosphorylations of 15 proteins, including Smad2/3, Erk1/2, Akt1/2/3, p38, p70S6k, GSK-3α/3β, HSP27, and so on, which were mainly involved in MAPK signaling pathway. These data demonstrated the effects of GDF11 on neural stem cell through the MAPK pathway.

2. Materials and methods

2.1. Agents

C17.2 neural stem cell line was purchased from zqxzbio (Shanghai, China). Dulbecco's modified Eagle's medium (DMEM), Penicillin-Streptomycin Solution and Trypsin were obtained from Hyclone (Logan, Utah, USA). Fetal bovine serum (FBS) and horse serum (HS) were purchased from Biological Industries (Beit Haemek, Israel). Recombinant human/mouse/rat GDF-11/BMP-11 and Phospho-MAPK proteome profiler array kit were obtained from R&D systems (Minneapolis, USA)). Dimethyl sulfoxide (DMSO), and superblock were purchased from Sigma-Aldrich (St. Louis, USA). NuPAGE LDS loading buffer and NuPAGE 4-12% Bis-Tris gel were obtained from Invitrogen (Waltham, USA). Phosphatase inhibitor cocktail and protease inhibitor cocktail were from MedChem Express (Shanghai, China). RIPA buffer was from Pierce (Rockford, USA). Rabbit anti-Smad2/3, rabbit anti-p-smad2(Ser465/467)/Smad3(Ser423/425), rabbit anti-CREB, rabbit anti-p-CREB (Ser133), rabbit anti-ERK, rabbit anti-p-ERK(Thr202/Tyr204), rabbit anti-p38, rabbit anti-p-p38(Thr180/Tyr182), rabbit anti-nestin, rabbit anti-βIII-tubulin, rabbit anti-GFAP, rabbit anti-β-actin, rabbit anti-GAPDH and goat anti-rabbit IgG were obtained from Cell Signal Technology (Beverly, MA, USA). Enhanced Cell Counting Kit-8 (CCK-8) and BCA Protein Assay Kit were obtained from Beyotime Biotechnology (Beijing, China). Enhanced chemiluminescence (ECL) was form Pierce (Rockford, USA).

2.2. C17.2 cell culture

C17.2 cells were cultured on 25-cm^2 culture flasks in complete medium (DMEM supplemented with 10% (v/v) FBS, 5% (v/v) HS, 100 units/ml penicillin and 100 μg/ml streptomycin) at 37 ^oC, 5% CO^2 in a humidified atmosphere. Media were changed every 2–3 days. After reaching 70-80% confluence, C17.2 cells were trypsinized and re-seeded at a density of $4*10^4$ cells/mL in complete medium which was changed to starved medium (DMEM supplemented with 0.5% HS and 1% FBS) one day post seeding. After 6 h of serum starvation, GDF11 was added at different concentrations indicated (0, 12.5, 25, 50 and 100ng/mL, respectively).

2.3. Cell morphology, viability, proliferation and apoptosis assay

C17.2 cells were seeded onto the 24-well plates at a density of $4*10^4$ cells/well in 0.1 mL complete medium. After adherence, complete medium was replaced with starved medium for 6h. The time of treatment and indicated concentrations of GDF11 were shown in corresponding figures. GDF11-untreated cells were served as control.

The cell morphology and viability were examined using LIVE/DEAD® viability/cytotoxicity kit for mammalian cells (Invitrogen, USA) according to the manufacturer instructions under inverted fluorescence microscope (AXIO, Zeiss, Jena, Germany). The live cells were stained with calcein AM in green, and the dead cells were stained with ethidium homodimer-1(EthD-1) in red.

Cell viability was assessed by CCK-8 assay, as well. Briefly, 10 μL of CCK-8 agent was added to each well before 2 h of the experiment termination. The optical density (OD) values

measured at 450 nm were determined using SpectraMax M2^e (Molecular Devices, Sunnyvale, USA). Then, by comparing the absorbance of GDF11-treated and untreated cells, percentage viability was calculated.

For proliferation assay, $1*10^4$/mL cells were cultured on 12-well plates in triplicates. When the cell cultured to 70–80% confluence (generally 3 days), cells were trypsinized and manually counted using a haemocytometer. Cell population doubling (PD) was calculated using the following formulae:

$$(1) PD = \log 2\ (N/N_0),$$

where N_0 represents the number of cells seeded at the initial passage, N is the final number of cells.

To investigate the apoptosis-inducing effect of GDF11, we identified apoptotic and necrotic cells by Annexin V-FITC and propidium iodide (PI) dual staining using FACScan flow cytometry (Becton-Dickinson, USA). Approximately $1*10^5$ cells were analyzed in each experimental group. The cell populations were distinguished according to their positioning of quadrants: live cells (Annexin V−/PI−), early/primary apoptotic cells (Annexin V+/PI−), late/secondary apoptotic cells (Annexin V+/PI+) and necrotic cells (Annexin V−/PI+).

2.4. Scratch wound healing assay

C17.2 cells were cultured with complete medium in a 48-well plate at a density of 5×10^4 cells/well. After reaching70-80% confluence, a single uniform scratch was made by using a 200μL pipette tip along the center of each monolayer. The scratch was lightly washed with PBS twice to remove the detached cells, and then starved medium supplemented with various concentrations of GDF11 was added (0ng/mL, 12.5ng/mL, 25ng/mL,50ng/mL and 100ng/mL, respectively). The scratches were monitored at 0h, 12h and 36h after scratching by taking photos with inverted microscope to measure the wound closure. The wound closures of various treatments at different time points were calculated with Image J software.

2.5. RNA extraction and qRT-PCR analysis

C17.2 cells were cultured on 12-well plates at a density of $4*10^4$ cells per well under standard conditions. Upon reaching 80% confluence, the complete medium was changed to starved medium. After 6 h of serum starvation, plates were treated with either indicated concentrations of GDF11 (25ng/mL, 50ng/mL and 100ng/mL, respectively) or vehicle in starved medium for 4h. Total RNA was extracted from the cultured cells using TRIZOL reagent according to the standard procedure. Total RNA (1μg) was reverse transcribed in a final volume of 20 μL in a reaction containing random primers, using iScriptTM cDNA Synthesis kit (Bio-Rad, Hercules, USA). qRT-PCR was done using the Quantitect SYBR Green PCR kit (Qiagen) with a ABI StepOnePlus Real-time PCR system (Applied Biosystems, Foster City, USA). Relative expression was calculated using the $2^{-\triangle\triangle Ct}$ method by normalizing with GAPDH housekeeping

gene expression and presented as fold changes relative to control. The primers for qRT-PCR were synthesized by Beijing Genomics Institute (Shenzhen, China) and the details of primer sequences are shown in Supplementary Table S1.

2.6. Phospho-proteome profiling array

Human phospho-MAPK array kit was used to determinate the relative levels of phosphorylation of mitogen-activated protein kinases (MAPKs) and other serine/threonine kinases with or without GDF11 treatment. Briefly, C17.2 cells were rinsed with PBS and solubilized with Lysis Buffer 6 (provided in Human Phospho-MAPK Array Kit) at $1*10^7$ cells/mL. After rocking gently at 2-8°C for 30 min, the lysates were centrifuged at 14,000 g for 5 min, and the supernate was collected and quantified the protein concentrations using BCA protein assay. The arrays were blocked by Buffer 5 for 1h on a rocking platform shaker. Afterwards, the mixture of sample and detection antibody cocktail were introduced and incubated overnight at 2-8°C on a rocking platform shaker. The following day, the membranes were washed three times, and then were incubated in streptavidin-HRP for 30 min followed by three washes. The protein blots were developed by ECL reagents. Densitometry analysis was measured with the Quantity One software, and the averaged intensity was calculated by subtracting the averaged background signal. The fold change was obtained by comparing GDF11-treated samples with the untreated control (indicated as a value of 1):

$$\text{Fold change} = \text{average intensity}_{(\text{GDF11-treated})} / \text{average intensity}_{(\text{control}).}$$

The respective coordinates of all the antibodies on the arrays and the corresponding phosphorylation sites can be found in “Supplementary Table S2”.

2.7. Western Blot analysis and validation

C17.2 cells were cultured in 6-well dishes in starved medium with or without GDF11 for 24h. Then, the cells were lysed in RIPA buffer containing 1× phosphatase inhibitor cocktail and 1× protease inhibitor cocktail on ice for 30 min, and centrifuged at 14000 g for 5 min at 4 ℃. The supernatants were collected, and the protein concentration was determined by BCA protein assay kit. The samples were mixed with 4× NuPAGE LDS loading buffer, separated on NuPAGE 4-12% Bis-Tris gels, and subsequently transferred to polyvinylidene difluoride membranes by a wet transfer apparatus (Bio-Rad, Hercules, USA). Following blocking with superblock at room temperature for 2h, the membranes were incubated with rabbit anti-β-actin (1:1000), anti-Smad2/3 (1:1000), anti-p-Smad2/3 (1:1000), anti-CREB (1:1000), anti-p-CREB (1:1000), anti-ERK (1:1000), anti-p-ERK(1:1000), anti-p38, anti-p-p38(1:1000), anti-nestin(1:1000), anti-βIII-tubulin(1:1000), anti-GFAP(1:1000) and anti-GAPDH, respectively, at 4℃ overnight. After washing with PBS supplemented with 0.1% Tween 20 (PBST), membranes were incubated with horseradish peroxidase-conjugated goat anti-rabbit IgG (1:3000) at room temperature for 2h, and were visualized by ELC reagents. The ImageJ software was used for densitometric analyses of

the blots.

2.8. Bioinformatic analyses

To further understand the functions and features of the identified and quantified proteins, we annotated functions and features of proteins from several different categories, including subcellular localization, domain, Gene Ontology (GO) and pathway.

We used WoLF PSORT (a subcellular localization predication tool, version of PSORT/PSORT II) and SubLoc (http://www.bioinfo.tsinghua.edu.cn/SubLoc/) were used to predict subcellular localization of all identified differentially expressed proteins.

The domain functional description of the differentially expressed proteins were annotated by InterProScan (a sequence analysis application) based on protein sequence alignment method, and the InterPro domain database was used (http://www.ebi.ac.uk/interpro/).

GO annotation was derived from the UniProt-GOA database (http://www.ebi.ac.uk/GOA/). And the differentially expressed proteins were classified by GO annotation based on the three categories (GO term level 1): biological process, cellular component and molecular function. According to GO annotation information of the identified proteins, we summed up the amount of the differentially expressed proteins in each GO term of level 2.

The protein-protein interaction networks and pathways were annotated by Kyoto Encyclopedia of Genes and Genomes (KEGG) database. KEGG pathways mainly including six categories: metabolism, genetic information processing, environmental information processing, cellular processes, organismal systems and human diseases.

2.9. Statistical analysis

The results were presented as the mean ± standard deviation (SD). Multi-group comparisons were performed by one-way ANOVA followed by Tukey's post hoc test. Paired analysis of control and treatment was accomplished using two-tailed unpaired or unpaired Student's *t* –tests when appropriate. In addition, Statistical analyses were conducted using SPSS statistics software,version 17.0 (SPSS Inc., Chicago, USA), and $p < 0.05$ was considered statistically significant..

3. Results

3.1. The positive and negative effects of GDF11 on cellular viability and proliferation

When compared with the quantity of C17.2 cells initially seeded, both GDF11- and vehicle-treated cells significantly proliferated after 72h of cultivation (Supplementary Fig. S1). Imaging revealed that GDF11 significantly altered the morphology of C17.2 cells (Fig.1a). Cells without GDF11 treatment remained their native neural stem cell state (Fig.1a, control), whereas cells treated with various concentrations of GDF11 showed visual outgrowth of neuritis, displaying phenotypes similar to neuronal and astrocytic-like cells (Fig.1a, GDF11). Moreover, supplement

with high concentrations of GDF11 (50 and 100 ng/mL) significantly resulted in morphological changes, differentiation and apoptosis, compared to the control (Supplementary Fig.S1a).

To investigate the effect of GDF11 on cell viability, C17.2 cells were treated with indicated concentrations of GDF11 (0, 12.5, 25, 50 and 100 ng/mL) for a 72h period, followed by CCK-8 assays. GDF11 slightly increased (less than 10%, $p<0.05$) cell viability after 24h treatment, whereas it did not significantly affect the cell viability after 72h treatment (Fig.1c).

As displayed in Fig.1d, all groups of C17.2 cells showed robust proliferation for the 6-passage duration. GDF11 showed no effect on C17.2 cell proliferation till the 4th passages. From the 5th passage, the low concentrations of GDF11 (12.5 and 25 ng/mL) still didn't affect the proliferation of C17.2 cells, however, presence of higher concentrations of GDF11 (50 and 100 ng/mL) significantly inhibited cell proliferation ($p<0.05$). And the exposure of C17.2 cells to 100 ng/mL GDF11 resulted in the lowest cumulative population doubling level during the 6 passages of cultivation amongst the 5 groups, which was approximately 17% lower than control ($p<0.05$).

Next, we detected the mRNA expression of cyclin D1 and cyclin D2, the cell cycle-related proteins. GDF11-treatment slightly but not significantly attenuated the expression of cyclin D1 and cyclin D2 in the mRNA levels (Fig. 2d; $p>0.05$). These provide a potential molecular basis for the effects of GDF11 on C17.2 cell viability and proliferation.

Together, these results revealed that GDF11 slightly increased cell viability after a short-term (24h) cultivation and showed no effect on cell viability from 1st to 4th passage of cultivation (approximately 10 days), however exposure of C17.2 cells to high levels of GDF11 for a long-term significantly suppressed cumulative population doubling.

3.2. GDF11 induced differentiation and apoptosis of C17.2 cells

The mRNA levels of the neural progenitor cell marker, nestin, were noticeably decreased after being treated with GDF11, as compared to control levels (Fig. 2a; $p<0.01$). By contrast, the GDF11-treated groups showed significant increases in βIII-tubulin (neuronal biomarker) and GFAP (astrocytic biomarker) mRNA expression as compared to the control (Fig. 2a; $p<0.05$). These all indicated the maturation and differentiation of C17.2 neural stem cells. The differences in nestin mRNA expression among the groups of GDF11 treatment were, however, not significant, similar to βIII-tubulin and GFAP. Concomitantly with the mRNA expression, the protein levels of nestin, βIII-tubulin and GFAP confirmed the similar results by western blot (Fig. 2b and c). When compared with the control, the GDF11-treated cells showed that the protein level of nestin was significantly attenuated whereas βIII-tubulin and GFAP were pronounced up-regulated (Fig. 2b and c), further indicating that GDF11 induced neuronal and astrocytic differentiation. However, no dose-dependent effect of GFD11 was observed.

The results of Annexin V-FITC/PI dual staining revealed that GDF11 substantially induced apoptosis of C17.2 cells. As shown in Fig. 1b and e, the number of total (both early and late) apoptotic cells significantly increased in a GDF11 dose-dependent manner. After 72h of cultivation, the apoptotic cells were negligible in C17.2 cells without GDF11-treated, whereas

there were 2.1%, 9.8%, 13.1% and 17.7% of cells exhibiting apoptosis as a result of exposure to 12.5, 25, 50 and 100ng/mL GDF11, respectively ($p<0.05$). Meanwhile, the amount of necrotic cells showed a slight but significant increase when treated with GDF11.

3.3. GDF11 suppressed the migration for C17.2 cells

The migration of C17.2 cells was performed by a "scratch wound healing'' assay. The wound closure data are shown in Fig.3. It was observed that the wound closure increased as cell migration progressed over time. After 12 h, the wound area had little difference compared to the initial scratch area. As compared with 0h, wound area of 36h that was still uncovered by migrating C17.2 cells significantly decreased, displaying 25.1% (0 ng/mL GDF11), 64.9% (12.5 ng/mL GDF11), 60.4% (25 ng/mL GDF11), 70.9% (50 ng/mL GDF11) and 75.7% (100 ng/mL GDF11) wound area, respectively (Fig.3b). That implied wound closure was significantly inhibited when cells were treated with GDF11**.** Of note, it was revealed that GDF11 showed slight but significant dose-dependent effects in the inhibition of the migration. Together, these results suggested that GDF11 significantly suppressed (but not completely abolished) the migratory potential of C17.2 neural stem cells.

3.4. GDF11 activated phosphorylation levels of selected signaling kinases

We deduced that, in C17.2 cells, GDF11 transmitted signals through phosphorylation of Smads, as GDF11 belongs to TGF-β superfamily. First of all, we analyzed the effects of GDF11 on TGF-β signal pathway (the classical pathway activated by TGF-β family members) in C17.2 neural stem cells. GDF11 showed no effect on both the mRNA and protein levels of Smad3 (Fig.2e and Fig.4a). For Smad2, GDF11 significantly up-regulated the transcriptional level other than the protein level (Fig.2e and Fig.4a). As shown in Fig.4a, cells untreated with GDF11 (control) displayed negligible phosphorylation of Smad2 and Smad3. On the contrary, presence of GDF11 pronouncedly induced Smad2 and Smad3 phosphorylation ($p<0.05$). However, this induction didn't reveal dose-dependent effects of GDF11. Next, we investigated the mRNA levels of receptors of TGF-β superfamily, activin type IIB receptor (ActRIIB) and the type I receptors, activin receptor-like kinase 5 (ALK5). The results of qRT-PCR revealed that GDF11 didn't alter mRNA expression of ActRIIB and ALK (Fig.2e).

In order to further determine the signal pathways affected by GDF11, we compared the phosphorylation levels of MAPKs in C17.2 cells treated with vehicle or GDF11 using a phospho-MAPK array kit. The fold changes were calculated from the ratio of intensity of the MAPK array from the GDF11 treated C17.2 cells to the control (untreated cells). Cut-off values were set 1.5-fold for up-regulated expression and 0.67-fold for down-regulated expression of a protein. We observed significant increases in the phosphorylation levels of a number of proteins in cells that were cultured with GDF11 when compared with the untreated cells (Fig.5, Supplementary Table S2 and Supplementary Fig.S2). Overall, 50% (13/26) proteins showed significantly increased phosphorylation after treatment with GDF11, whereas the phosphorylation levels of the remaining 50% (13/26) were still unchanged. Strikingly, when

treated with GDF11, there were no proteins that showed decreased phosphorylation. In addition, the differentially expressed proteins that showed the most significant increases included Creb (3.42 times increased), HSP27 (3.05 fold increased), Akt1/2/3 (2.55-, 2.47- and 1.50-fold increased expression, respectively), GSK-3β and GSK3α/β (2.12- and1.50 -fold increased, respectively), p38 α/β (3.21 and 1.73 times increased), Erk1 (1.57), MKK3/6 (2.03- and 1.52-fold increased, respectively) and p70s6k (1.93 times increased) (Fig.5c and Supplementary Fig.S2; $p<0.05$). These indicated that GDF11 activated the MAPK/Erk and p38 MAPK pathways but not JNK pathway in C17.2 neural stem cells. Remarkably, many of these differentially expressed proteins are involved in signal transductions of cell survival and apoptosis.

3.5. Functional Classification of Differentially Expressed Proteins

As shown in Table 1, the differentially expressed proteins were mainly classified as cytoplasmic (n=8), nuclear (n=7) and mitochondrial (n=1) proteins.

For an overview of the differentially expressed proteins, GO annotation was carried out to identify the significantly enriched GO functions. According to the analysis, the 15 differentially expressed proteins between GDF11-treated cells and control were mainly clustered into 38 functional groups, including 18 biological processes, 12 cellular components, and 8 molecular functions (Fig.6a).

Biological process category according to GO annotations indicated that all the 15 differentially expressed proteins were involved in metabolic process. And other significant function groups included cellular process (13/15), response to stimulus (13/15), signaling (13/15) and localization (12/15), etc (Fig.6a).

In the category of cellular components, the differentially expressed proteins were mainly involved in cell (13/15), organelle (14/15), cytoplasm (12/15) and nucleus (13/15), indicating the similar subcellular localization that was obtained from WoLF PSORT (Table 1). Not only the similarities but also differences were found between the cellular component category and subcellular localization results. According to the functional analysis of GO annotation, we found six proteins were involved in plasma membrane, however, no membrane-associated proteins were observed from subcellular localization results.

The most representative of molecular function category was “binding”, which accounted for all the 15 differentially expressed proteins. And most of the differentially expressed proteins were also related to catalytic activity (11/15), transferase activity (11/15) and kinase activity (11/15). These results also elucidated that the related signal pathways activated by GDF11.

3.6. KEGG Enriched Pathways

To explore the potential mechanisms for GDF11-mediated cell behavior (cellular proliferation, differentiation, apoptosis and migration) in C17.2 neural stem cells, we used the KEGG database to determine the protein-protein interaction networks and pathways involved in the up-regulated phosphoproteins. The 15 differentially expressed proteins were mainly mapped to 51 pathways

according to the KEGG database, which were mainly associated with environmental information processing (signal transduction), organismal systems (immune system, nervous system, endocrine system and ageing), cellular processes (cell growth and death, transport and catabolism, and cellular community) and human diseases (drug resistance, endocrine and metabolic diseases, neurodegenerative diseases, infectious diseases, and cancers) (Supplementary Table S3). These all indicated the differentially expressed proteins were mainly involved in signal transduction of cellular behavior. Furthermore, domain functional description of the differentially expressed proteins annotated by InterProScan, were significantly enriched in protein kinase domain (25.58%) and protein kinase-like domain (25.58%) (Fig.6b). These were also in line with the results of molecular function category of GO annotation which indicated the differentially expressed proteins were mainly in connection with catalytic activity, transferase activity and kinase activity (Fig. 6a).

A major overlapping network was enriched in this analysis (Fig.6c). Three canonical signaling pathways (TGF-β, PI3K-Akt and MAPK signaling pathways), that were activated by the up-regulation of phosphoproteins, were identified, and the cross-talking signaling cascade was shown as well. One mainly functional cluster was apparent in the protein-protein interaction, including Akt1/2/3 (the key components in the PI3K-Akt signal pathway), Erk1 (the key components of MAPK/Erk pathway) and p38α/β (the key components in the p38 MAPK signal pathway). These results provided a possible resource for future studies of the proteins involved in GDF11-treated C17.2 cells.

3.7. Validation of selected differentially expressed proteins

To confirm the results of phospho-MAPK array, three differentially expressed protein candidates (Creb, p38 and Erk) were selected for further validation using western blot. Total protein lysates from C17.2 cells cultured with indicated concentrations of GDF11 (0, 12.5, 25, 50 and 100 ng/ml, respectively) were prepared and the phosphorylation levels were determined by their respective phosphorylated antibodies. When compared with control, however, no detectable changes in total Creb, p38 or Erk protein expression were observed in GDF11-treated C17.2 cells. Nevertheless, GDF11-treatment significantly increased the phosphorylation levels of Creb, p38 and Erk (Fig.4b, c and d; all $p < 0.05$). These western blot results were generally consistent with the results of the phospho-MAPK array.

4. Discussion

Around the world, the number of older people is precipitously increasing. Therefore, searching for anti-ageing or rejuvenating factors is quite important for developing therapeutic strategies for the treatment of age-related diseases. Recently, it was suggested that GDF11 was a potential rejuvenating factor, which not only reversed age-related cardiac hypertrophy and dysfunction in skeletal muscle in mouse(Loffredo et al. 2013; Poggioli et al. 2016; Sinha et al. 2014), but also induced rejuvenation of impairments in cognitive function of ageing mouse by remodeling the cerebral vascular and enhancing neurogenesis(Katsimpardi et al. 2014). Similar phenomenon

was validated in human by a prospective cohort study, that higher levels of GDF11/8 were associated with lower risk of cardiovascular events and death in patients with stable ischaemic heart disease(Olson et al. 2015). However, these initial findings have been challenged by later recent studies. Egerman and colleagues(Egerman et al. 2015) discovered GDF11 supplementation inhibited muscle regeneration and decreased satellite cell expansion in mice, and implied that GDF11 was not a rejuvenation factor but a potential target for pharmacologic blockade to treat age-related sarcopenia. Hinken et al.(Hinken et al. 2016) also suggested GDF11 wasn't a rejuvenator of aged murine skeletal muscle satellite cells. In addition, others reported restoring GDF11 in old mice showed no effect on pathological hypertrophynovelty (Smith et al. 2015).

Because GDF11 was reported to improve neurogenic rejuvenation, we hypothesized that GDF11 would influence the cellular behavior of C17.2 neural stem cells, including viability, proliferation, differentiation, apoptosis and migration. Therefore, we focused on the effects and potential mechanism of action of GDF11 on viability, proliferation, differentiation, apoptosis and migration in C17.2 cells. Here, our results indicated that GDF11 substantially induced differentiation and apoptosis, and suppressed migration of C17.2 cells mainly through MAPK signal pathway. Meanwhile, GDF11 exhibited sight but significant increase in cellular viability in a short time of growth (24h), and showed no effects on cellular viability for medium-term cultivation (< 4 passages; approximately 10 days). However, long-term cultured (> 4 passages) with high concentrations of GDF11 significantly inhibited the proliferation of C17.2 cells (Fig. 1c and d; $p<0.05$). To the best of our knowledge, we are unaware of any similar published results. Strikingly, similar to our results, it was found that GDF11 slightly increased cell viability after short-term treatment and slightly decreased cell viability after long-term treatment in human umbilical vein endothelial cells(Zhang et al. 2016). Previously, it was suggested that GDF11 acted as a negative regulator of neurogenesis(Wu et al. 2003). Recently, Williams *et al*. (Williams et al. 2013) reported a controversial finding that that GDF11 suppressed proliferation and migration of Cor-1 cells, whereas no effect on differentiation was observed. The conflicting results may be caused by GDF11 from different vendors, different batches of GDF11 from the same manufacturer, or cells from different sources, etc.

As a member of TGF-β superfamily, it was reported that GDF11 activated TGF-β signal pathway as a consequence of phosphorylating Smad2/3 in several cell types(Liu et al. 2016; Loffredo et al. 2013; Zhang et al. 2016). In the present study, we successfully observed GDF11 induced phosphorylation of Smad2/3 in C17.2 neural stem cells. Consistent with our results, it was also confirmed that Cor-1 neural stem cell line was able to respond to GDF11 stimulation by Smad2/3 phosphorylation(Williams et al. 2013). It is widely known that the Smad2/3-dependent TGF-β signals have been implicated in the proliferation and differentiation of neural stem cell. For example, GDF11 negatively regulated self-renewal of neuroepithelial stem cells through TGF-β signals(Falk et al. 2008).

Proteins, not genes, are the specific practitioners of cellular life activities. Although genome and transcriptome analyses are very useful to reveal the mechanism of GDF11

stimulation, proteomic profiles may not be accurately predicted by transcriptome profiling due to several factors, such as post-translational modifications. Therefore, research on proteomics is helpful to provide new information concerning the C17.2 cells response to GDF11 stimulation. Based on phospho-proteome profiling array and bioinformatic analysis (Figs.5 and 6), we found 15 differentially expressed proteins, including p38, Erk, Akt, GSK3α/β, Creb, MKK3/6, p70S6k and HSP27, which were mainly involved in signal transductions of cell survival and apoptosis. Besides TGF-β signal pathway, we also found Akt pathway and two important MAPK pathways (MAPK/Erk and p38 MAPK pathways) were activated, but not JNK pathway. Similarly, it also reported GDF11 activated TGF-β/Smad2/3, whereas suppressed JNK signaling pathways in apolipoprotein E-null mice(Mei et al. 2016). The functions of MAPK/Erk and p38 MAPK pathways are complex, which are involved in controlling cell proliferation, differentiation, survival/apoptosis and migration(Wagner & Nebreda 2009). Various studies demonstrated MAPK/Erk pathway was involved in cellular proliferation and migration(Khodosevich 2009; Wu et al. 2014). Although p38 MAPK pathway is normally associated with anti-proliferative and apoptotic functions(Wagner & Nebreda 2009), it is also reported that p38 is implicated in pro-survival functions, including positively regulate proliferation, differentiation and anti-apoptosis(Halawani et al. 2004; Ricote et al. 2006; Terriente-Félix et al. 2017; Thornton et al. 2008). MAPK/Erk, Akt and p38 MAPK pathways were required for the migration of cortical neurons upon HGF stimulation(Segarra et al. 2006), however, we observed GDF11 significantly suppressed the capacity of C17.2 neural stem cells to migrate with the activation of Erk MAPK, PI3K/Akt andp38 MAPK pathways. Of the 15 differentially expressed proteins we identified, HSP27 and p70S6K are two important downstream effecters of Akt pathway. Mechanistically, PI3K/Akt activates the phosphorylation of HSP27 p70s6k, which facilitates protein folding and controls protein synthesis, to inhibit apoptosis and promote proliferation(Khodosevich 2009; Li et al. 2008; Rane et al. 2003). All of these suggested that GDF11 regulated the proliferation, differentiation, apoptosis and migration of C17.2 cells by cross-talking with MAPK signaling pathway.

Neuronal migration is a complex and key process in physiological and pathological conditions. Increasing the quantity of nerve cells and the migration of neurons to the final position are critical to reverse age-related dysfunction in brain(Contreras-Vallejos et al. 2012; Martino et al. 2011; Zhao et al. 2008). It should be noted that, although GDF11-treatment for 24h slightly decreased the viability of C17.2 cells (Fig.1c), it did not significantly induce cell death (Fig. S1b). GDF11 showed no effect on cell viability after 72h cultivation (Fig.1c), however, it significantly stimulated cell death (Fig.S1a). In addition, we found GDF11 significantly suppressed the migration of C17.2 cells. Despite the fact that GDF11 indeed induced C17.2 cells to differentiate into neurons and astrocytes, our point of view is that it should be cautious if GDF11 is considered as a rejuvenated factor for neural stem cells.

5. Conclusion

In the present study, it revealed that GDF11 was an important regulator of neural stem cell. In

C17.2 neural stem cells, GDF11 seemed to have a positive effect on cell viability after 24h treatment but showed a tendency for negative effect for long-term cultivation. In addition, GDF11 significantly induced differentiation and apoptosis, and suppressed migration of C17.2 neural stem cells. Further analysis of the activity that occurs downstream of MAPK signaling, which is activated by GDF11, may clarify the potential mechanism of action by which the cellular behavior was induced. Taken together our current findings implied that GDF11 might be a potential target for pharmacologic blockade instead of a rejuvenated factor for neural stem cells.

Acknowledgements

The authors are grateful for helpful comments of bioinformatic analyses from Jingjie PTM BioLab (Hangzhou) Co. Ltd (China).

References

Contreras-Vallejos E, Utreras E, and Gonzalez-Billault C. 2012. Going out of the brain: non-nervous system physiological and pathological functions of Cdk5. *Cellular signalling* 24:44-52.

Egerman Marc A, Cadena Samuel M, Gilbert Jason A, Meyer A, Nelson Hallie N, Swalley Susanne E, Mallozzi C, Jacobi C, Jennings Lori L, Clay I, Laurent G, Ma S, Brachat S, Lach-Trifilieff E, Shavlakadze T, Trendelenburg A-U, Brack Andrew S, and Glass David J. 2015. GDF11 Increases with Age and Inhibits Skeletal Muscle Regeneration. *Cell Metabolism* 22:164-174. 10.1016/j.cmet.2015.05.010

Falk S, Wurdak H, Ittner LM, Ille F, Sumara G, Schmid M-T, Draganova K, Lang KS, Paratore C, and Leveen P. 2008. Brain area-specific effect of TGF-β signaling on Wnt-dependent neural stem cell expansion. *Cell stem cell* 2:472-483.

Halawani D, Mondeh R, Stanton L-A, and Beier F. 2004. p38 MAP kinase signaling is necessary for rat chondrosarcoma cell proliferation. *Oncogene* 23:3726-3731. 10.1038/sj.onc.1207422

Hinken AC, Powers JM, Luo G, Holt JA, Billin AN, and Russell AJ. 2016. Lack of evidence for GDF11 as a rejuvenator of aged skeletal muscle satellite cells. *Aging cell* 15:582-584.

Katsimpardi L, Litterman NK, Schein PA, Miller CM, Loffredo FS, Wojtkiewicz GR, Chen JW, Lee RT, Wagers AJ, and Rubin LL. 2014. Vascular and Neurogenic Rejuvenation of the Aging Mouse Brain by Young Systemic Factors. *Science* 344:630-634. 10.1126/science.1251141

Khodosevich K. 2009. Major signaling pathways in migrating neuroblasts. *Frontiers in Molecular Neuroscience* 2:7. 10.3389/neuro.02.007.2009

Li W, Tan D, Zhang Z, Liang JJ, and Brown RE. 2008. Activation of Akt-mTOR-p70S6K pathway in angiogenesis in hepatocellular carcinoma. *Oncology reports* 20:713-719.

Liu W, Zhou L, Zhou C, Zhang S, Jing J, Xie L, Sun N, Duan X, Jing W, Liang X, Zhao H, Ye L, Chen Q, and Yuan Q. 2016. GDF11 decreases bone mass by stimulating osteoclastogenesis and inhibiting osteoblast differentiation. *Nature Communications* 7:12794. 10.1038/ncomms12794

Loffredo FS, Steinhauser ML, Jay SM, Gannon J, Pancoast JR, Yalamanchi P, Sinha M, Dall'Osso C, Khong D, Shadrach JL, Miller CM, Singer BS, Stewart A, Psychogios N, Gerszten RE, Hartigan AJ, Kim M-J, Serwold T, Wagers AJ, and Lee RT. 2013. Growth Differentiation Factor 11 Is a Circulating Factor that Reverses Age-Related Cardiac Hypertrophy. *Cell* 153:828-839. 10.1016/j.cell.2013.04.015

528 Martino G, Pluchino S, Bonfanti L, and Schwartz M. 2011. Brain regeneration in physiology and pathology: the
529 immune signature driving therapeutic plasticity of neural stem cells. *Physiological reviews* 91:1281-1304.
530 Mei W, Xiang G, Li Y, Li H, Xiang L, Lu J, Xiang L, Dong J, and Liu M. 2016. GDF11 protects against endothelial injury
531 and reduces atherosclerotic lesion formation in apolipoprotein E-null mice. *Molecular Therapy* 24:1926-
532 1938.
533 Oh SP, Yeo C-Y, Lee Y, Schrewe H, Whitman M, and Li E. 2002. Activin type IIA and IIB receptors mediate Gdf11
534 signaling in axial vertebral patterning. *Genes & development* 16:2749-2754.
535 Olson KA, Beatty AL, Heidecker B, Regan MC, Brody EN, Foreman T, Kato S, Mehler RE, Singer BS, and Hveem K.
536 2015. Editor's choice: Association of growth differentiation factor 11/8, putative anti-ageing factor, with
537 cardiovascular outcomes and overall mortality in humans: analysis of the Heart and Soul and HUNT3
538 cohorts. *European Heart Journal* 36:3426.
539 Pepinsky B, Gong B-J, Gao Y, Lehmann A, Ferrant J, Amatucci J, Sun Y, Bush M, Walz T, Pederson N, Cameron T, and
540 Wen D. 2017. A Prodomain Fragment from the Proteolytic Activation of Growth Differentiation Factor 11
541 Remains Associated with the Mature Growth Factor and Keeps It Soluble. *Biochemistry* 56:4405-4418.
542 10.1021/acs.biochem.7b00302
543 Poggioli T, Vujic A, Yang P, Macias-Trevino C, Uygur A, Loffredo FS, Pancoast JR, Cho M, Goldstein J, Tandias RM,
544 Gonzalez E, Walker RG, Thompson TB, Wagers AJ, Fong YW, and Lee RT. 2016. Circulating Growth
545 Differentiation Factor 11/8 Levels Decline With AgeNovelty and Significance. *Circulation Research* 118:29-
546 37. 10.1161/circresaha.115.307521
547 Rane MJ, Pan Y, Singh S, Powell DW, Wu R, Cummins T, Chen Q, McLeish KR, and Klein JB. 2003. Heat Shock Protein
548 27 Controls Apoptosis by Regulating Akt Activation. *Journal of Biological Chemistry* 278:27828-27835.
549 10.1074/jbc.M303417200
550 Ricote M, García-Tuñón I, Bethencourt F, Fraile B, Onsurbe P, Paniagua R, and Royuela M. 2006. The p38
551 transduction pathway in prostatic neoplasia. *The Journal of Pathology* 208:401-407. 10.1002/path.1910
552 Santos R, Wu J, Hamilton JA, Pinter R, Hindges R, and Calof AL. 2012. Restoration of Retinal Development in Vsx2
553 Deficient Mice by Reduction of Gdf11 Levels. *Advances in experimental medicine and biology* 723:671-677.
554
555 Segarra J, Balenci L, Drenth T, Maina F, and Lamballe F. 2006. Combined Signaling through ERK, PI3K/AKT, and
556 RAC1/p38 Is Required for Met-triggered Cortical Neuron Migration. *Journal of Biological Chemistry*
557 281:4771-4778. 10.1074/jbc.M508298200
558 Sinha M, Jang YC, Oh J, Khong D, Wu EY, Manohar R, Miller C, Regalado SG, Loffredo FS, and Pancoast JR. 2014.
559 Restoring systemic GDF11 levels reverses age-related dysfunction in mouse skeletal muscle. *Science*
560 344:649-652.
561 Smith SC, Zhang X, Zhang X, Gross P, Starosta T, Mohsin S, Franti M, Gupta P, Hayes D, Myzithras M, Kahn J, Tanner
562 J, Weldon SM, Khalil A, Guo X, Sabri A, Chen X, MacDonnell S, and Houser SR. 2015. GDF11 Does Not
563 Rescue Aging-Related Pathological HypertrophyNovelty and Significance. *Circulation Research* 117:926-
564 932. 10.1161/circresaha.115.307527
565 Terriente-Félix A, Pérez L, Bray SJ, Nebreda AR, and Milán M. 2017. A Drosophila model of myeloproliferative
566 neoplasm reveals a feed-forward loop in the JAK pathway mediated by p38 MAPK signalling. *Disease*
567 *Models & Mechanisms* 10:399-407. 10.1242/dmm.028118
568 Thornton TM, Pedraza-Alva G, Deng B, Wood CD, Aronshtam A, Clements JL, Sabio G, Davis RJ, Matthews DE, Doble

B, and Rincon M. 2008. Phosphorylation by p38 MAPK as an Alternative Pathway for GSK3 Inactivation. *Science* 320:667-670. 10.1126/science.1156037

Wagner EF, and Nebreda ÁR. 2009. Signal integration by JNK and p38 MAPK pathways in cancer development. *Nature Reviews Cancer* 9:537-549. 10.1038/nrc2694

Walker RG, Czepnik M, Goebel EJ, McCoy JC, Vujic A, Cho M, Oh J, Aykul S, Walton KL, Schang G, Bernard DJ, Hinck AP, Harrison CA, Martinez-Hackert E, Wagers AJ, Lee RT, and Thompson TB. 2017. Structural basis for potency differences between GDF8 and GDF11. *BMC Biology* 15:19. 10.1186/s12915-017-0350-1

Walker RG, Poggioli T, Katsimpardi L, Buchanan SM, Oh J, Wattrus S, Heidecker B, Fong YW, Rubin LL, Ganz P, Thompson TB, Wagers AJ, and Lee RT. 2016. Biochemistry and Biology of GDF11 and MyostatinResponse to Walker et al. *Circulation Research* 118:1125-1142. 10.1161/circresaha.116.308391

Williams G, Zentar MP, Gajendra S, Sonego M, Doherty P, and Lalli G. 2013. Transcriptional Basis for the Inhibition of Neural Stem Cell Proliferation and Migration by the TGFβ-Family Member GDF11. *PLoS ONE* 8:e78478. 10.1371/journal.pone.0078478

Wu H-H, Ivkovic S, Murray RC, Jaramillo S, Lyons KM, Johnson JE, and Calof AL. 2003. Autoregulation of Neurogenesis by GDF11. *Neuron* 37:197.

Wu X-S, Wang X-A, Wu W-G, Hu Y-P, Li M-L, Ding Q, Weng H, Shu Y-J, Liu T-Y, Jiang L, Cao Y, Bao R-F, Mu J-S, Tan Z-J, Tao F, and Liu Y-B. 2014. MALAT1 promotes the proliferation and metastasis of gallbladder cancer cells by activating the ERK/MAPK pathway. *Cancer Biology & Therapy* 15:806-814. 10.4161/cbt.28584

Zhang Y-H, Cheng F, Du X-T, Gao J-L, Xiao X-L, Li N, Li S-L, and Dong D-L. 2016. GDF11/BMP11 activates both smad1/5/8 and smad2/3 signals but shows no significant effect on proliferation and migration of human umbilical vein endothelial cells. *Oncotarget* 7:12063.

Zhao C, Deng W, and Gage FH. 2008. Mechanisms and functional implications of adult neurogenesis. *Cell* 132:645-660.

Figure 1

Effect of GDF11 on C17.2 cells.

(a) The representative images of live and dead cell staining. C17.2 cells were cultured with indicated concentrations of GDF11. Images were obtained at 200X magnification by inverted fluorescence microscope. The live cells were stained with calcein AM in green, and the dead cells were stained with EthD-1 in red. (b) GDF11 induced apoptosis in C17.2 neural stem cells. C17.2 cells were treated with vehicle or GDF11 (12.5, 25, 50 and 100ng/mL) for 48h and cell distribution was analysed using Annexin V-FITC and PI dual staining. The FITC and PI fluorescence was measured by flow cytometer with FL-1 and FL-2 filters, respectively. Lower left quadrant-- live cells (Annexin V−/PI−), lower right quadrant--early/primary apoptotic cells (Annexin V+/PI−), upper right quadrant--late/secondary apoptotic cells (Annexin V+/PI+) and upper left quadrant--necrotic cells (Annexin V−/PI+). (c) The viability of C17.2 cells after 24h or 72h of cultivation with various concentrations of GDF11 or vehicle was measured using CCK-8 method.. N=3, $p<0.05$. (d) Cumulative population doubling levels of C17.2 cells supplemented with different GDF11 concentrations for a total period of 6 passages. N=4, *$p<0.05$ compared with control. (e) Quantitative analyses of the GDF11 effect on apoptosis. N=3, *$p<0.05$versus with vehicle control and **$p<0.01$versus with vehicle control.

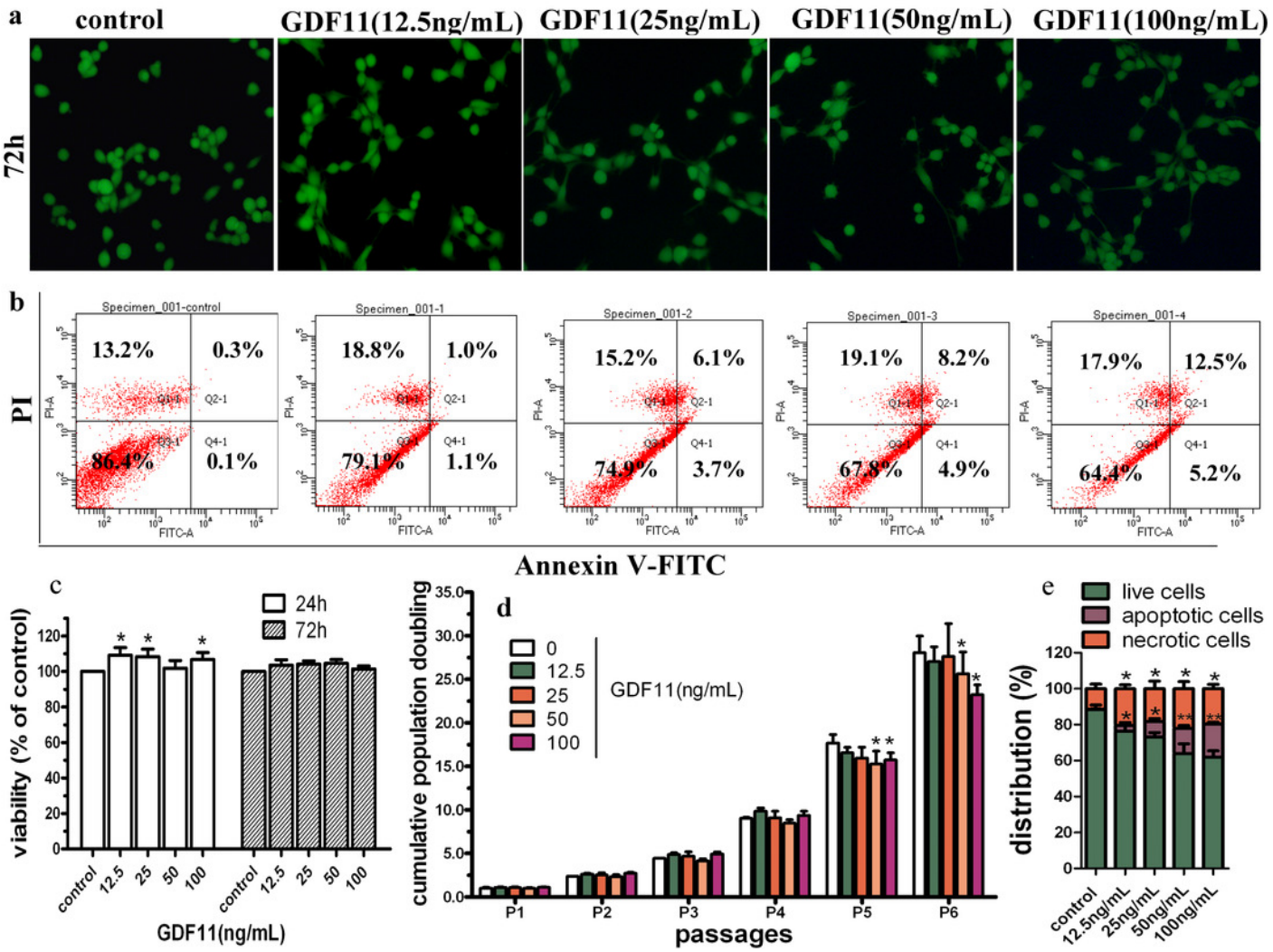

Figure 2

The effect of GDF11 on mRNA and protein expression

(a) Nestin, βIII-tubulin and GFAP mRNA levels of C17.2 cells after GDF11 or vehicle (control) treated for 5h.The results display mean ± SD of n= 4 and were analysed by one-way ANOVA followed by Tukey's post hoc test. *p< 0.05 as compared with mRNA levels in control cells. (b) Nestin, βIII-tubulin and GFAP protein levels of C17.2 cells after GDF11 (50ng/mL, "T") or vehicle ("C") treated for 72h. (c) Quantitative analyses of protein expression in relation to β-actin expression. Results were analysed by Student's t-test. N=6, *p< 0.05. (d) Cyclin D1, Cyclin D2 and EGFR mRNA expression after GDF11 or vehicle treated for 5h. N=5, *p< 0.05 and **p<0.01. (e) The mRNA levels of Smad2, Smad3, Alk5 and ActRIIB after GDF11 or vehicle treated for 5h. N=5, *p< 0.05 and **p<0.01.

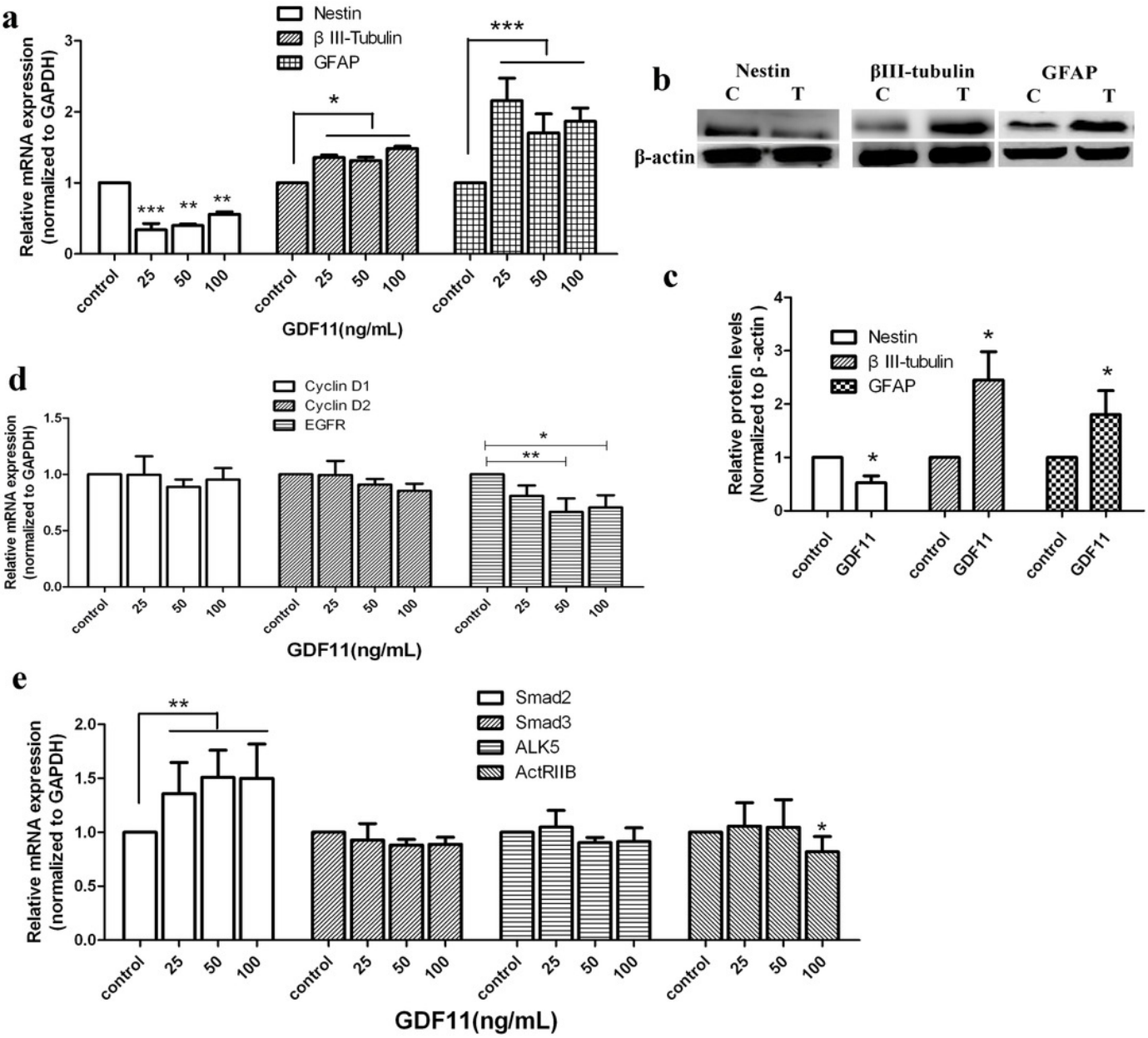

Figure 3

GDF11 inhibited the migration of C17.2 cells

Scratch-wound closure was monitored over time. (a) Representative images showed that GDF11 induced significantly decreased migration speed compared with control (GDF11 untreated cells). Black lines in each graph were pointed toward wound edges. (b) Quantification of the remaining wound area uncovered by migrating C17.2 cells revealed a significant inhibition of migration in GDF11-treated cells. The scratch wound areas at time point 0 hour were set to 100%, and the wound areas at other time point were normalized to their respective 0 hours. Bar is 500 μm (n=5; *p<0.05).

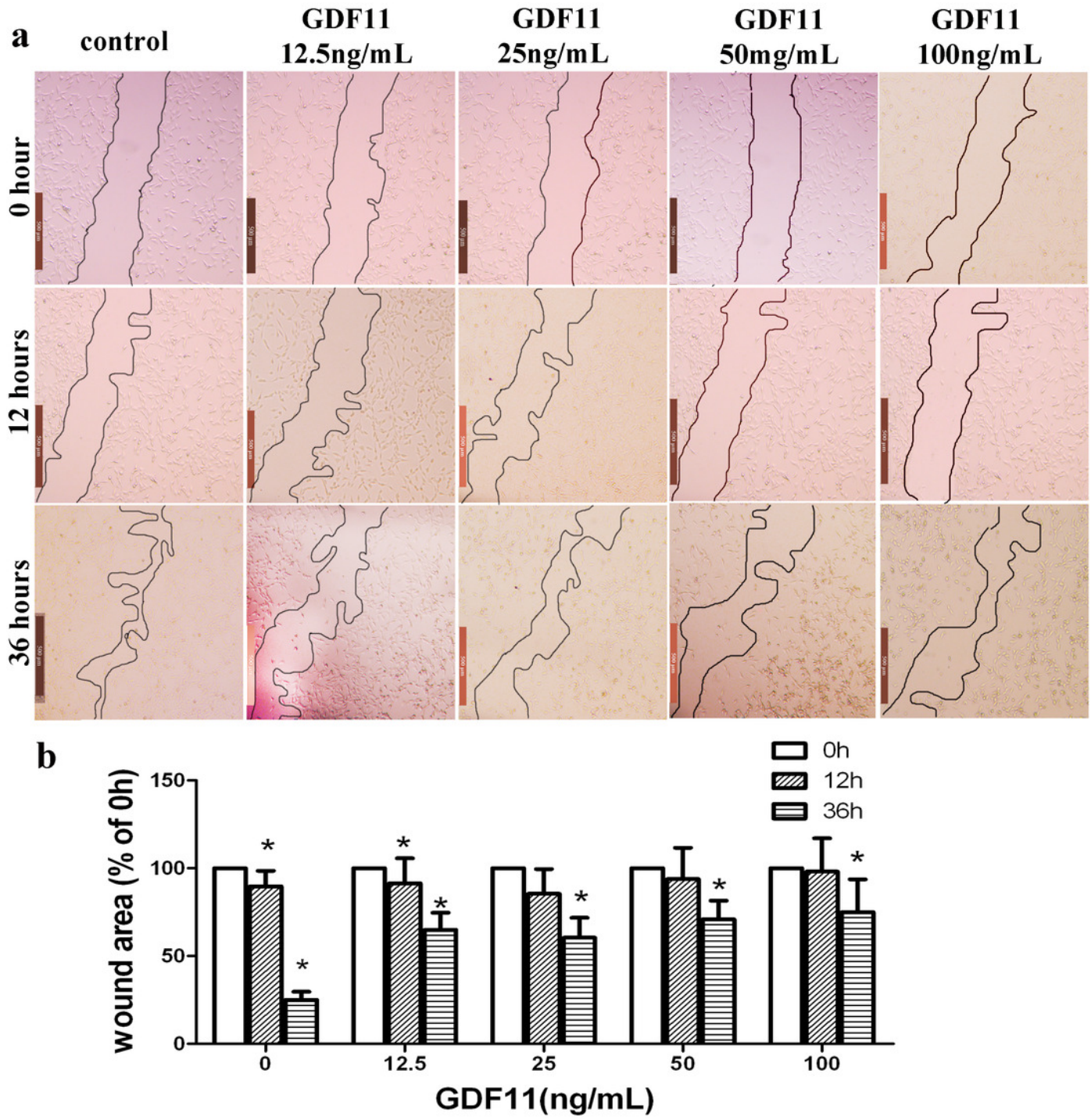

Figure 4

GDF11 increased the phosphorylation level of Smad2/3, Creb, p38 and Erk in C17.2 neural stem cells.

(a-d). After 24h cultivation, GDF11 showed no effect on total protein of Smad2/3, Creb, p38 and Erk, but significantly phosphorylated Smad2 (Ser465/467), Smad3(Ser423/425), Creb(Ser133), p38(Thr180/Tyr182) and Erk (Thr202/Tyr204) in C17.2 cells. N=4, *p< 0.05, **p<0.01 and ***p<0.001 when compared with control.

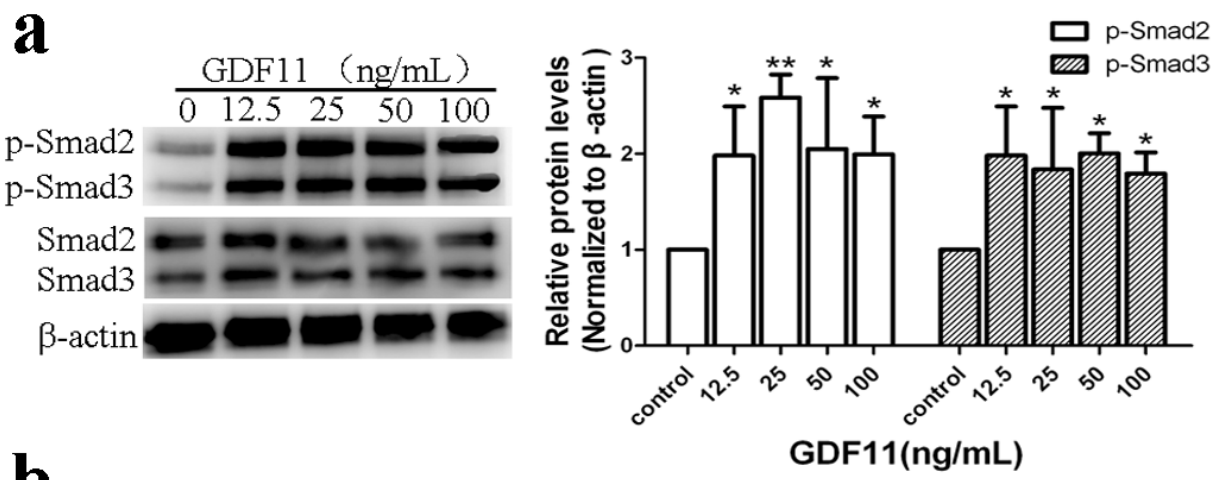

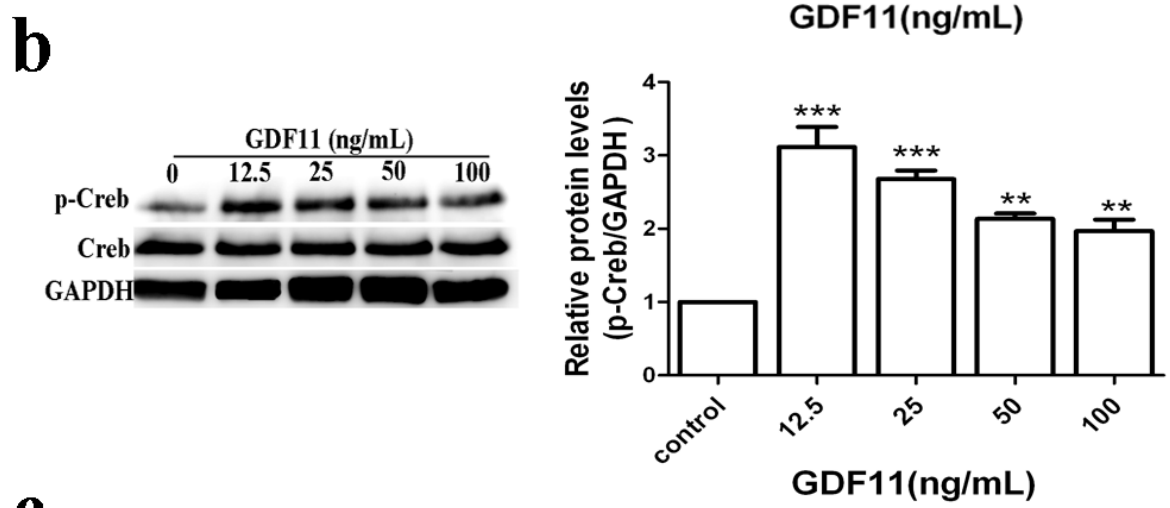

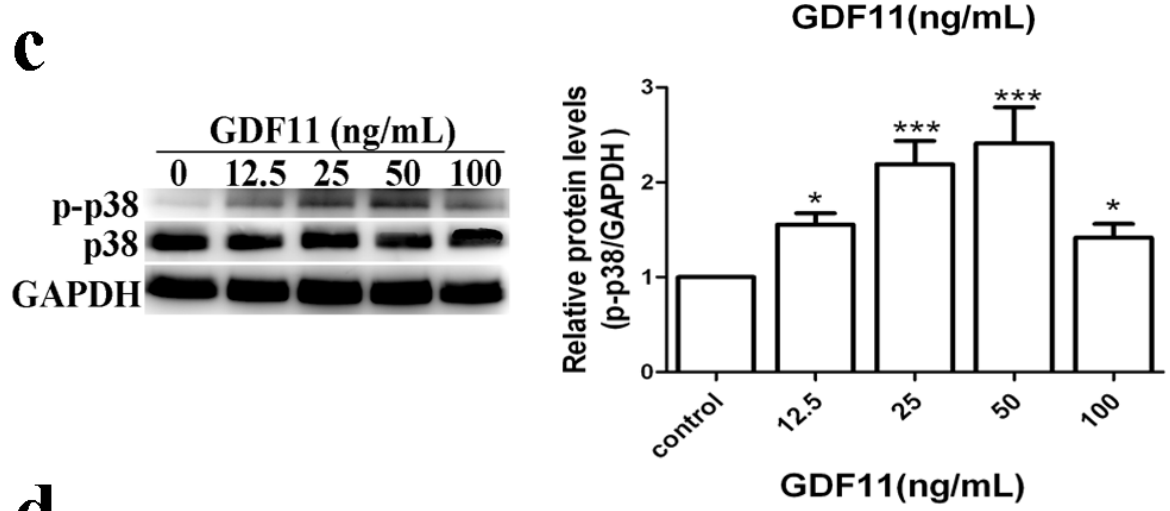

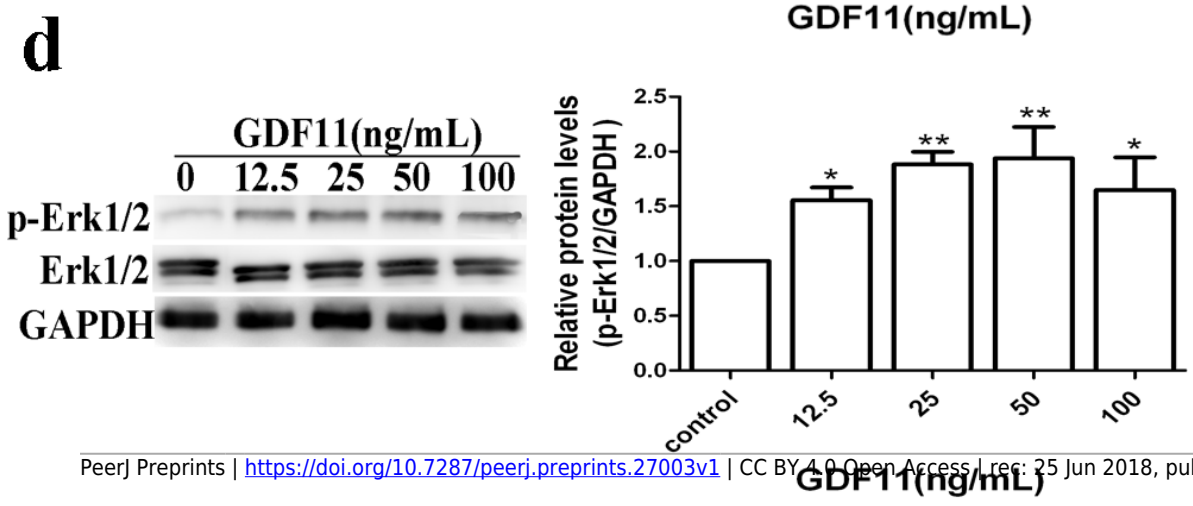

Figure 5

Alterations of MAPK pathway-related proteins in GDF11-treated C17.2 cells.

(a). Phosphoproteome profiling of C17.2 cells in response to GDF11 stimulation. Total cell lysates from C17.2 cells with25ng/mL GDF11- or vehicle-treated were incubated on membranes of the phospho-proteomics platforms (human Phospho-MAPK, 23 different MAPKs and other serine/threonine kinases), as described in “Materials and Methods”. (b). Human Phospho-MAPK array coordinates. (c). The graph shows the relative fold change of proteins with significant difference upon GDF11 treatment, setting 1 for control. Protein levels with higher than ± 1.5 folds indicated by dotted lines are considered as the differentially expressed proteins.

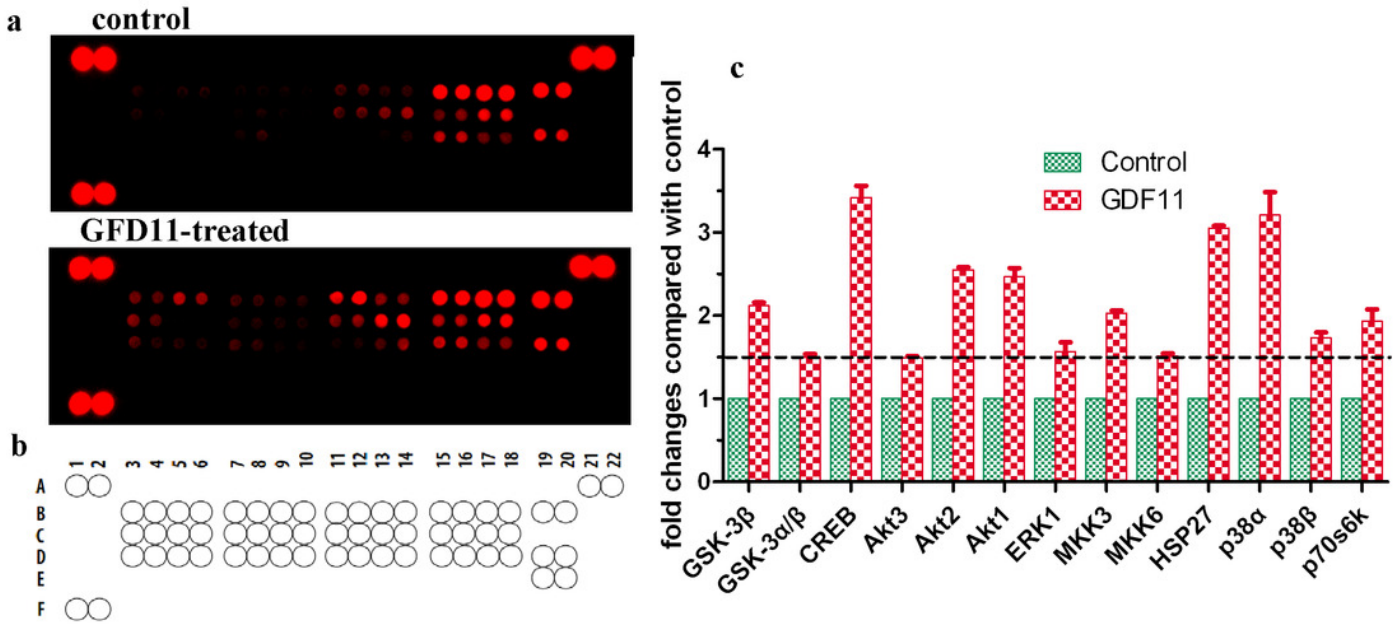

Figure 6

Functional classification and protein-protein interaction of the differentially expressed proteins in GDF11-treated C17.2 cells and control.

(a). According to GO annotation, the differentially expressed proteins between GDF11-treated cells and control were mainly clustered into 38 functional groups, including 18 biological processes, 12 cellular components, and 8 molecular functions. (b). Protein domain categories of the differentially expressed proteins were annotated by InterProScan. (c). The protein-protein interaction network of the differentially expressed proteins was analyzed by KEGG) database.

PeerJ Preprints | https://doi.org/10.7287/peerj.preprints.27003v1 | CC BY 4.0 Open Access | rec: 25 Jun 2018, publ: 25 Jun 2018

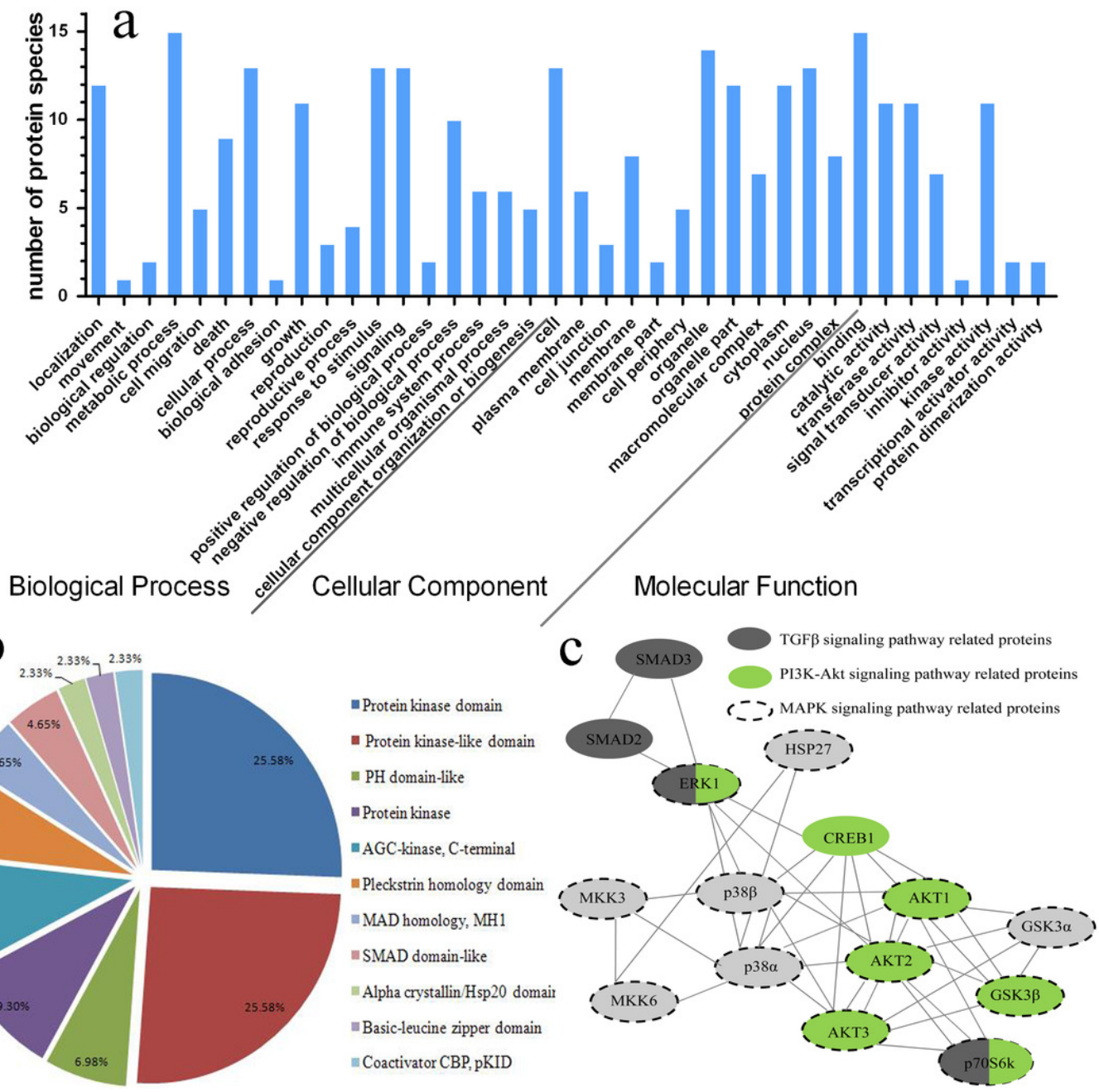

Table 1(on next page)

The subcellular location of the differentially expressed proteins

Table 1. The subcellular location of the differentially expressed proteins

Proteins	Subcellular Location	Fold Changes
GSK-3β	cytoplasm	2.12
GSK-3α	nucleus	1.50
CREB	nucleus	3.42
Akt2	cytoplasm	2.55
Akt1	cytoplasm	2.47
ERK1	cytoplasm	1.57
MKK3	nucleus	2.03
HSP27	nucleus	3.05
P38α	cytoplasm	3.21
p38β	cytoplasm, nucleus	1.73
p70s6k	nucleus	1.93
Smad2	mitochondria	1.99
Smad3	cytoplasm, nucleus	2.01
Akt3	cytoplasm	1.50
MKK6	cytoplasm	1.52